

Article

Pd₄S/SiO₂: A Sulfur-Tolerant Palladium Catalyst for Catalytic Complete Oxidation of Methane

Lei Ma ^{1,*}, Shiyuan Yuan ¹, Hanfei Zhu ¹, Taotao Jiang ¹, Xiangming Zhu ^{2,*}, Chunshan Lu ¹ and Xiaonian Li ^{1,*}

¹ Industrial Catalysis Institute, Laboratory Breeding Base of Green Chemistry-Synthesis Technology, Zhejiang University of Technology, Hangzhou 310014, China; yuanshiyan318420@163.com (S.Y.); hanfeizhu0701@foxmail.com (H.Z.); jiangtaotao2016@outlook.com (T.J.); lcszjcn@zjut.edu.cn (C.L.)

² Centre for Synthesis and Chemical Biology, UCD School of Chemistry, University College Dublin, Belfield, Dublin 4, Ireland

* Correspondence: malei@zjut.edu.cn (L.M.); xiangming.zhu@ucd.ie (X.Z.); xnli@zjut.edu.cn (X.L.); Tel.: +86-571-88320920 (L.M.)

Received: 4 April 2019; Accepted: 29 April 2019; Published: 30 April 2019



Abstract: Sulfur species (e.g., H₂S or SO₂) are the natural enemies of most metal catalysts, especially palladium catalysts. The previously reported methods of improving sulfur-tolerance were to effectively defer the deactivation of palladium catalysts, but could not prevent PdO and carrier interaction between sulfur species. In this report, novel sulfur-tolerant SiO₂ supported Pd₄S catalysts (5 wt. % Pd loading) were prepared by H₂S–H₂ aqueous bubble method and applied to catalytic complete oxidation of methane. The catalysts were characterized by X-ray diffraction, Transmission electron microscopy, X-ray photoelectron Spectroscopy, temperature-programmed oxidation, and temperature-programmed desorption techniques under identical conditions. The structural characterization revealed that Pd₄S and metallic Pd⁰ were found on the surface of freshly prepared catalysts. However, Pd₄S remained stable while most of metallic Pd⁰ was converted to PdO during the oxidation reaction. When coexisting with PdO, Pd₄S not only protected PdO from sulfur poisoning, but also determined the catalytic activity. Moreover, the content of Pd₄S could be adjusted by changing H₂S concentration of H₂S–H₂ mixture. When H₂S concentration was 7 %, the Pd₄S/SiO₂ catalyst was effective in converting 96% of methane at the 400 °C and also exhibited long-term stability in the presence of 200 ppm H₂S. A Pd₄S/SiO₂ catalyst that possesses excellent sulfur-tolerance, oxidation stability, and catalytic activity has been developed for catalytic complete oxidation of methane.

Keywords: sulfur-tolerance; Pd₄S; catalytic oxidation of methane; sulfur poisoning

1. Introduction

Methane as the main component of natural gas is playing an increasingly important role in the global energy structure [1,2]. Effective catalytic complete oxidation of CH₄ can improve combustion efficiency and reduce air pollutants, such as CO, NO_x, and unburned hydrocarbon [3–8]. It has therefore found great applications in modern industry, such as catalytic exhaust converters aimed to reduce methane emission and catalytic gas turbine combustors designed to combust fuel under mild conditions [9,10]. Supported PdO catalysts have shown excellent catalytic property in methane oxidation, and currently are under extensive study [11–18]. However, once sulfur species (e.g., H₂S or SO₂) are present in the reaction atmosphere, the poisoning of PdO catalyst which would lead to inactive PdO-SO_x is irreversible and the activity of the catalyst cannot be recovered at relatively low temperature [19–25].

Hence, many efforts have been devoted in the past decade to enhance sulfur resistance of supported PdO catalysts. Currently there are two primary approaches to improve the performance of palladium

catalysts against sulfur poisoning: the first is to use alkaline carriers (e.g., γ -Al₂O₃) and enhance their adsorption ability toward acidic sulfur species to protect the active phase of PdO [23,26,27], and the second is to introduce an extra active ingredient to form a catalyst system with dual activity, such as Pd–Pt complex, to avoid sulfur poisoning [24,28]. However, these methods can only defer the deactivation of palladium catalysts as neither the alkaline carrier nor the extra active ingredient can prevent the interaction between PdO and sulfur species. In other words, sulfur poisons would eventually encroach PdO and make it inactive. As such, these catalyst systems did not really possess the ability of sulfur-tolerance.

The research on sulfur-tolerant palladium catalyst system in methane catalytic oxidation reaction is rare and lack of substantial progress in the literature [20,26–28]. Therefore, development of a reliable sulfur-tolerant catalyst system seems to be of great importance. In view of the great potential of catalytic oxidation of methane, we decided to pursue a new catalytic system that could be of high tolerance of sulfur poisons. We speculated Pd_xS_y in combination with acidic carrier would be an ideal system for methane oxidation based on the following two points. First, it would be the best scenario for sulfur-tolerant catalysts that neither the support nor the palladium active phase itself could interact with sulfur species. Pd_xS_y and acidic carrier such as SiO₂ would likely meet the requirement. Second, seeing that sulfur and oxygen are located in the adjacent position of the same main group in the periodic table, i.e., the chalcogen group, the designed Pd_xS_y might possess similar catalytic activity to PdO.

In the literature, the majority of Pd_xS_y (Pd₄S, Pd₃S, Pd_{2.8}S, Pd₁₆S₇, PdS or PdS₂, etc.) were prepared by gas sulfuration with H₂S–H₂ [25,29–35]. Herein, we would like to present a new procedure for the preparation of Pd_xS_y/SiO₂ catalysts via aqueous bubble sulfuration of Pd/SiO₂ with H₂S–H₂ with varied H₂S concentration. Compared with the gas sulfuration, the aqueous bubble method was performed in much milder conditions. Besides the sulfur resistance and catalytic activity, the stability of Pd_xS_y/SiO₂ catalyst was the other focus of our investigation.

2. Results and Discussion

2.1. Fresh Catalysts

2.1.1. Catalyst Characterization

Freshly prepared catalysts were first tested by X-ray diffraction (XRD) as showed in Figure 1. The freshly prepared catalyst is named (fV), where V represents H₂S concentration. No other palladium species were found except for metallic Pd⁰. The sulfuration of Pd to form Pd₄S under H₂S–H₂ atmosphere was via the reaction: $4\text{Pd} + \text{H}_2\text{S} \leftrightarrow \text{Pd}_4\text{S} + \text{H}_2$ [36–40]. This reversible reaction meant that metallic Pd⁰ could not be fully sulfurized to Pd₄S. Therefore, it was reasonable to detect metallic Pd⁰ on the surface of freshly sulfurized catalyst. However, it was worth noting that the intensity of the diffraction peak of metallic Pd⁰ changed regularly with the increase of H₂S concentration. The average particle size of metallic Pd⁰ calculated by Scherrer formula was further shown in Table 1. With the increase of H₂S concentration, the change of average particle size of metallic Pd⁰ could be divided into three stages. They were gradually reduced (0 → 5%), stable (5% → 7%), and increased (7% → 10%). These results indicated the Pd/SiO₂ precursor had been changed by sulfuration.

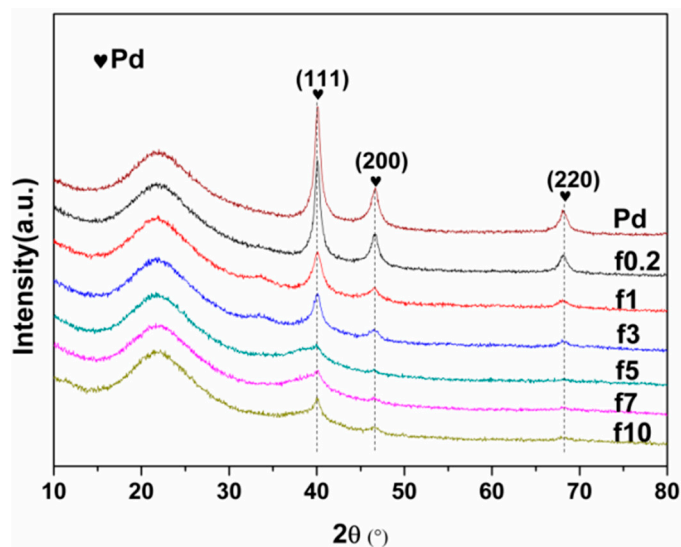


Figure 1. X-ray diffraction (XRD) patterns of freshly prepared catalysts sulfurized with different H_2S concentration.

Table 1. Average particles size of freshly prepared catalysts sulfurized with different H_2S concentration.

Catalyst	FWHM	Size (nm)
Pd	0.761	12.2
f0.2	0.803	11.5
f1	1.328	6.9
f3	1.297	6.7
f5	3.329	2.6
f7	3.262	2.6
f10	2.163	4.0

FWHM: full-width at half-maximum

Since XRD characterization could not directly provide evidence of the existence of Pd_xS_y , the freshly prepared catalysts were further characterized by high resolution transmission electron microscopy (HR-TEM) and illustrated in Figure 2. The lattice spacing distance of Pd species particles on freshly prepared catalyst are 0.225 nm and 0.245 nm, corresponding to the Pd(111) and $\text{Pd}_4\text{S}(102)$, respectively [JCPDS No. 73-1387, JCPDS No. 46-1043]. In addition to the metallic Pd(111), the $\text{Pd}_4\text{S}(102)$ was found on the surface of all the freshly prepared catalysts. The literature on the preparation of Pd_xS_y under $\text{H}_2\text{S}-\text{H}_2$ atmosphere showed that the Pd_4S with the highest proportion of Pd/S was the first Pd_xS_y species [38,41]. Therefore, it was reasonable to firstly form the Pd_4S under the condition of 60 °C aqueous bubble sulfuration.

The subsequent characterization by X-ray photoelectron spectroscopy (XPS) could provide further evidence for the existence of Pd_xS_y , as shown in Figure 3. After curve fitting analysis, the $\text{S}2\text{p}_{3/2}$ of freshly prepared catalyst could be deconvoluted into a large peak at 168.5 eV and a small peak at 165.1 eV, which corresponded to S^0 [42] and Pd_4S [42–44], respectively. With the increase of H_2S concentration, the XPS peak intensity of sulfur species increased gradually. At the same time, the $\text{Pd}3\text{d}_{5/2}$ could be deconvoluted into two peaks at ~335.6 eV and ~337.5 eV which corresponded to metallic Pd^0 [45,46] and Pd_4S [47,48], respectively. This indicated that Pd_4S and metallic Pd^0 were the primary palladium species on the freshly prepared catalysts. These results are in good agreement with the characterization results of XRD and HR-TEM. If the Pd_4S had similar properties to PdO , the amount of Pd_4S would be the key factor influencing the performance of the catalyst. The XPS data (Figure 3) were further analyzed to provide Table 2 that listed the composition ratio of palladium species of freshly prepared catalysts. It could be noted that the sulfuration process was the transition of metallic Pd^0 to Pd_4S . With the increase of H_2S concentration, the change of Pd_4S ratio could also be divided into

three stages. They were gradually increased (0 → 5%), stable (5% → 7%), and reduced (7% → 10%). Variation of metallic Pd⁰ content was opposite to that of Pd₄S. This variation was entirely consistent with the average particle size of metallic Pd⁰. It was obvious that the variation of the average particle size of metallic Pd⁰ was caused by the change of metallic Pd⁰ content on the catalyst surface.

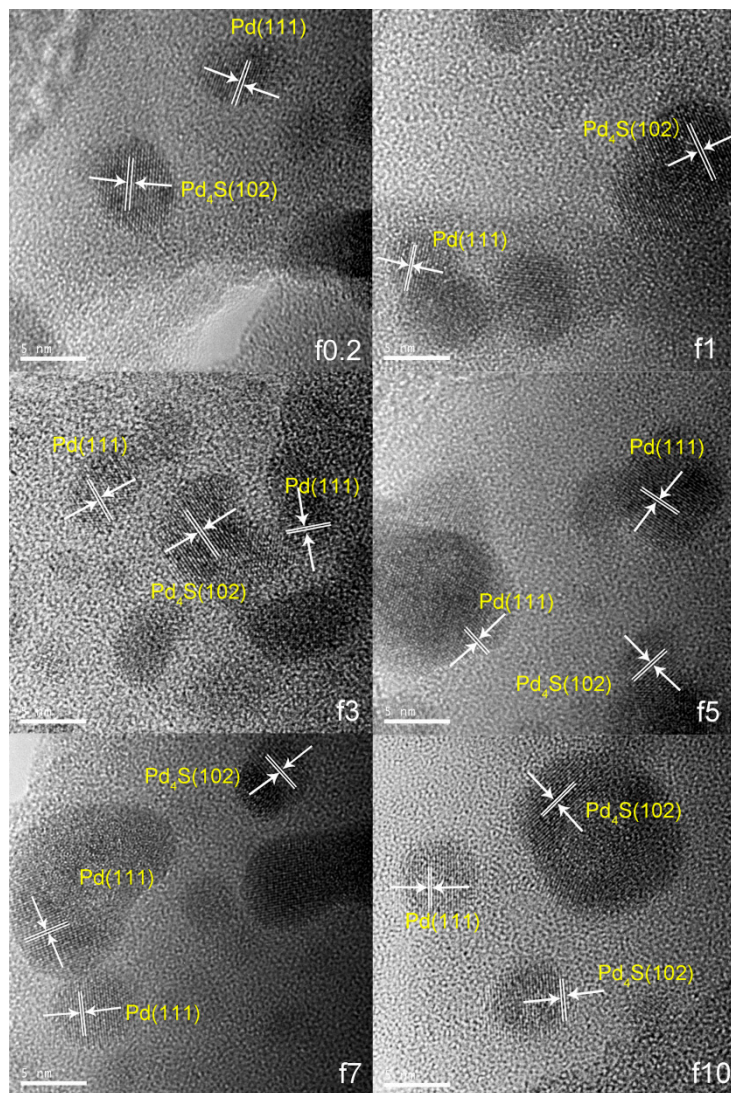


Figure 2. High resolution transmission electron microscopy (HR-TEM) images of freshly prepared catalysts with different H₂S concentration.

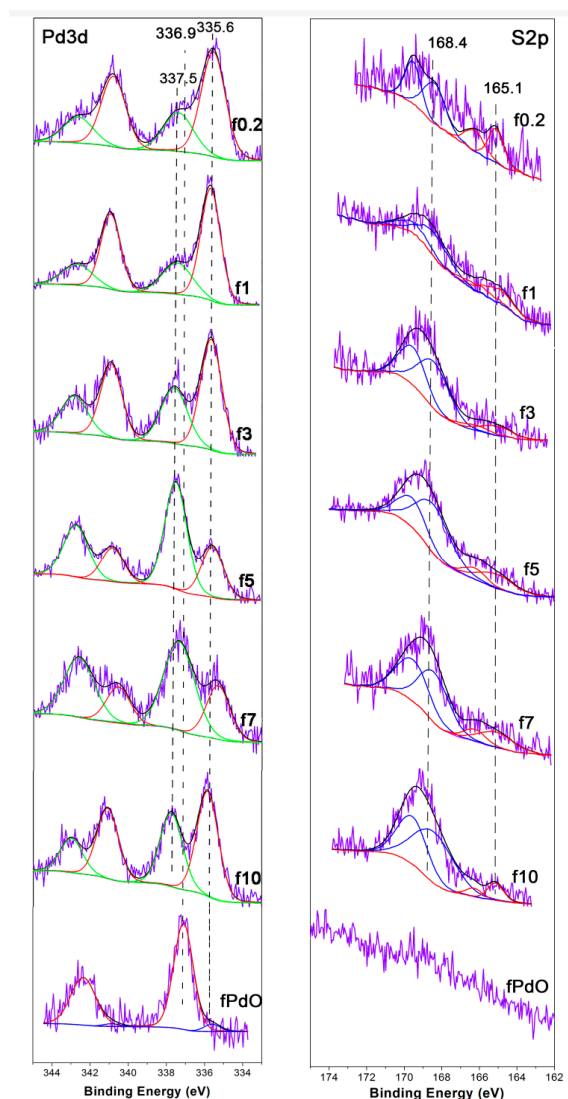


Figure 3. X-ray photoelectron spectroscopy (XPS) Pd3d and S2p of freshly prepared catalysts with different H₂S concentration.

Table 2. Palladium species content of freshly prepared catalysts with different H₂S concentration ^a.

Catalyst	Composition Ratio of Palladium Species (%)	
	Pd ⁰	Pd ₄ S
f0.2	68.9	31.1
f1	68.6	31.4
f3	61.6	38.4
f5	33.4	66.6
f7	32.1	67.9
f10	57.9	42.1

^a: Calculated by Pd fitted peak area by XPS.

2.1.2. Activity Studies

In order to test whether the Pd₄S possessed the desired sulfur-tolerance and catalytic activity, its catalytic property for methane oxidation in the presence of 200 ppm H₂S was then examined by measuring methane conversion against the reaction time at different reaction temperatures. As shown in Figure 4, when the temperature was 500 °C, the presence of H₂S had no impact on all the catalysts. However, once the reaction temperature dropped to 400 °C, the compared PdO/SiO₂ catalyst was

deactivated very rapidly. We estimated that at this temperature sulfur species could turn the active PdO into inactive PdO-SO_x species, which could then hardly decompose at low temperature [23,24,49]. In contrast, under the same conditions, all the catalysts prepared by our own procedure did not show any deactivation at 400 °C. This clearly stated that the combination of Pd₄S and SiO₂ was effective in resisting sulfur poisoning. At the same time, the activity of the catalyst with 7% H₂S concentration was even equal to that of PdO catalyst. This further stated that the combination of Pd₄S and SiO₂ had high enough catalytic activity. Furthermore, it was found that the methane conversion of all catalysts decreased to less than 10% at 370 °C. This dramatic decrease in catalytic activity was not due to sulfur poisoning, but the high reaction temperature required for methane activation [50–52]. Therefore, it was best to set the reaction temperature at 400 °C. This temperature could not only reflect the sulfur-tolerance, but also compare the catalytic activity.

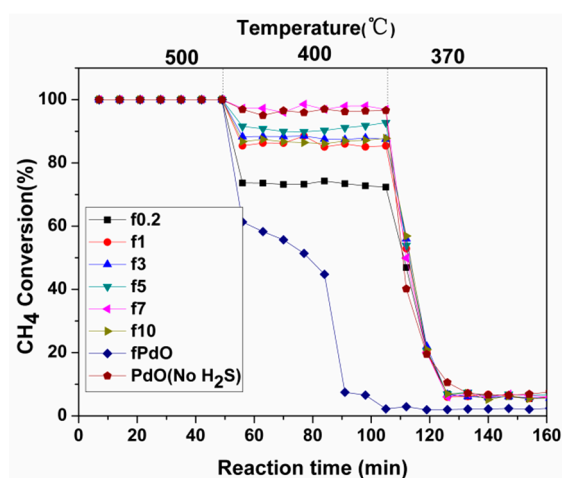


Figure 4. Catalytic performance of freshly prepared catalysts with different H₂S concentration. Gas composition: CH₄ (v% = 2%), O₂ (v% = 8%), H₂S (v% = 0.02%), and N₂ (v% = 89.8%); Flow rate = 200 mL/min; and GHSV (gas hourly space velocity) = 60000 mL/(g·h).

Meanwhile, it should be pointed out here that although all the sulfurized catalysts exhibited the similar sulfur-tolerance, the catalytic activity at 400 °C was not same. As the H₂S concentration increased from 0.2% to 7%, the catalytic activity increased gradually. However, when the H₂S concentration increased to 10%, the catalytic activity decreased. This variation was very similar to the variation of Pd₄S content on the surface of freshly prepared catalyst. However, we could not simply assume that catalytic activity depended solely on Pd₄S. The reason was that the stability of Pd₄S and metallic Pd⁰ on the surface of freshly prepared catalyst was still undiscovered under high reaction temperature and presence of oxygen. Under such reaction condition, metallic Pd⁰ was liable to be oxidized to PdO. Therefore, palladium species on the surface of freshly prepared catalyst might not be the true palladium species involved in the reaction. Next, we would characterize the used catalyst to determine the actual palladium species on the catalyst surface.

2.2. Used Catalyst

2.2.1. Catalyst Characterization

The XRD patterns of used catalysts were given in Figure 5. The used catalyst is named (uV), where V represents H₂S concentration. The characteristic diffraction peak attributed to sulfur species was found on the compared PdO/SiO₂ catalyst. However, no diffraction peaks attributed to sulfur species were found in all sulfurized catalysts after the reaction. The reason should be that the sulfurized catalyst had the ability to resist sulfur poisoning. Not surprisingly, almost all the diffraction peaks observed in the sulfurized catalyst were attributed to PdO after the reaction. A weak diffraction peak of metallic Pd⁰ could be observed only when H₂S concentration was 0.2%. This implied that most of

the metallic Pd⁰ on the freshly prepared catalyst had been oxidized to PdO under reaction conditions. However, the above results did not show whether the most important Pd₄S remains stable during the reaction and this needed to be identified by other characterization.

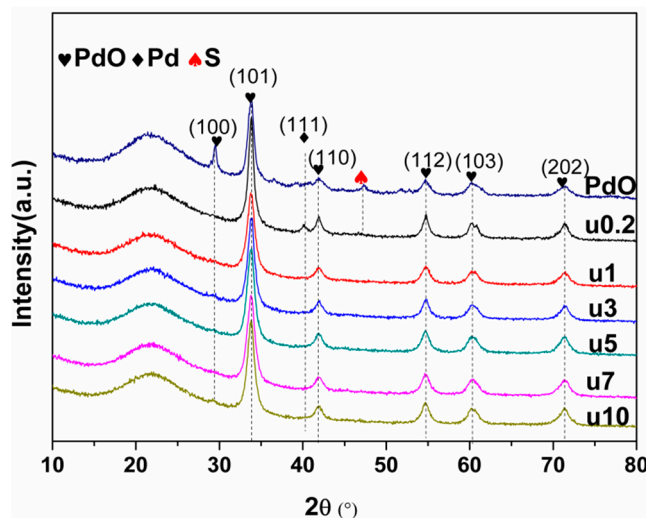


Figure 5. XRD patterns of used catalysts with different H₂S concentration.

The presence of PdO confirmed our previous speculation that the palladium species on the surface of freshly prepared catalysts were not entirely stable during the vigorous oxidation reaction. However, XRD characterization could only reveal that PdO species were formed during the reaction of freshly prepared catalysts. However, whether the essential Pd₄S species could stably exist in large quantities would be the main factor affecting the sulfur-tolerance of the catalyst. Figure 6 shows HR-TEM images of the used catalysts. It could be found that the palladium species on the surface of the used catalyst were more complicated than the freshly prepared catalyst. Figure 6 clearly indicates that in addition to Pd⁰(111), PdO(101) and PdO(110) also appeared in large numbers on the surface of all the used catalysts [JCPDS No.06-0515]. At the same time, the most interesting thing was that Pd₄S(102) species could be found on all catalyst surfaces. This indicated that the Pd₄S species could remain stable during the high temperature and high oxygen reaction of methane oxidation.

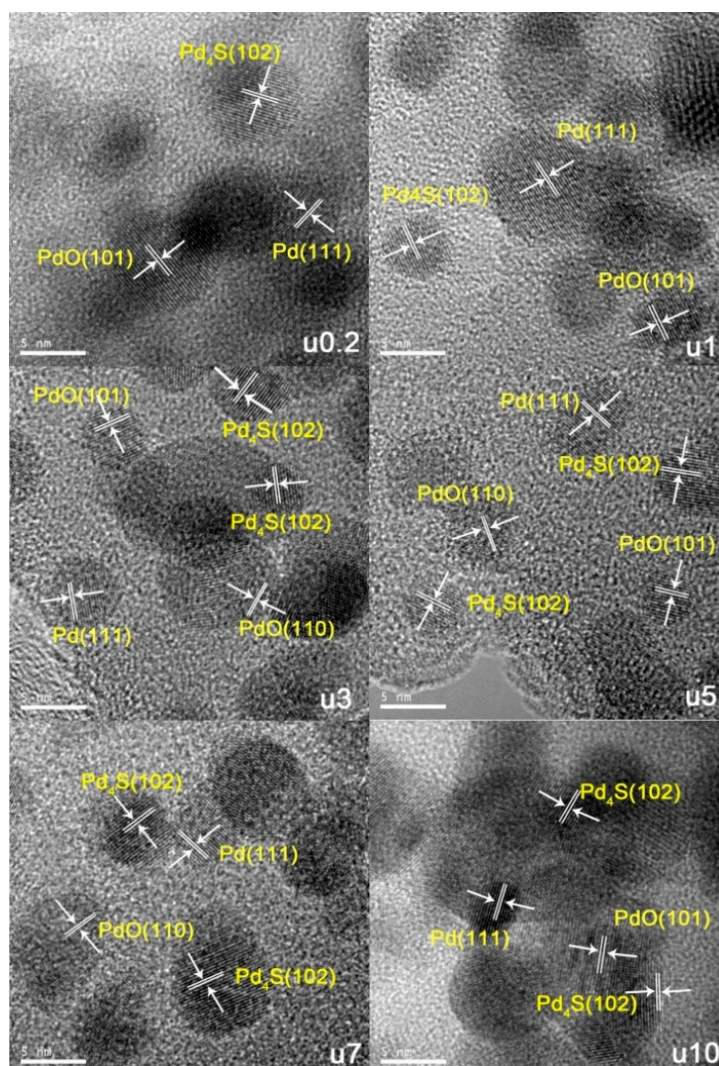


Figure 6. HR-TEM images of the used catalysts with different H_2S concentration.

Owing to the lack of data on the relative content of PdO on the surface of used catalyst, when Pd_4S and PdO coexist, we could not distinguish whether Pd_4S and PdO affect the catalytic activity alone or in combination. Therefore, used catalysts were further analyzed by XPS characterization, as shown in Figure 7. After curve fitting analysis, the $\text{Pd}3d_{5/2}$ could be deconvoluted into three peaks at ~ 337.5 eV, ~ 336.9 eV, and ~ 335.6 eV, which were assigned to Pd_4S [47,48], PdO [48], and metallic Pd^0 [45,46], respectively. The above characterization results revealed the fact that under the reaction conditions, the actual palladium species on the used catalyst surface should be Pd_4S , PdO, and metal Pd^0 . At the same time, the S2p peak attributed to S^0 was not observed (see Figure 3), only the very weak S2p peak attributed to Pd_4S could be observed. In contrast, the Pd3d peak at ~ 337.3 eV and S2p peak at 168.1 eV of used PdO/ SiO_2 could be attributed to PdO- SO_x . This comparison results indicated that Pd_4S could protect other palladium species from sulfur poisoning.

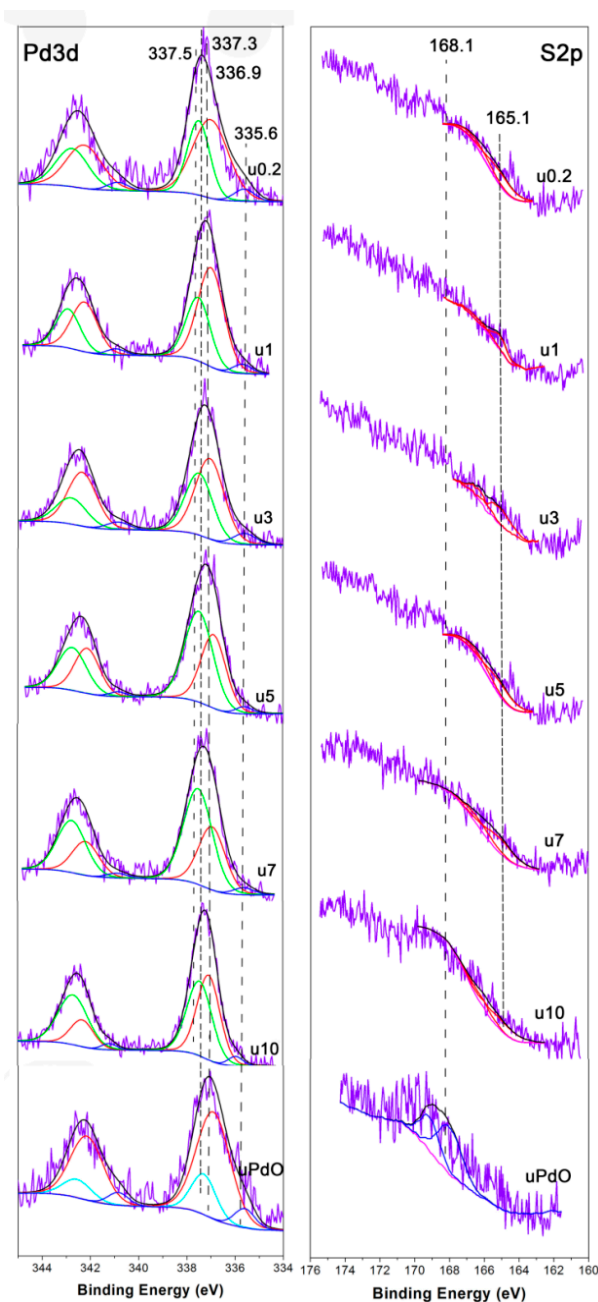


Figure 7. XPS Pd3d and S2p of the used catalysts with different H₂S concentration.

Table 3 listed the composition ratio of palladium species of used catalysts. Compared with the relative content of palladium species on the surface of fresh catalyst (Table 1), it could be noted that a large number of PdO species appeared on the surface of the used catalyst, while the Pd⁰ content of the metal decreased significantly. This was clearly the oxidation of metal Pd⁰ to PdO during the reaction. At the same time, the relative content of Pd₄S was basically stable during the reaction. This indicated that the PdO formed during the reaction was mainly derived from the metal Pd⁰, but not derived from Pd₄S. Temperature-programmed Oxidation (TPO) of fresh Pd/SiO₂, f7 and u7 catalysts with the same mass was investigated by thermogravimetric analysis. The oxidation stability of the catalyst was examined by recording the mass change in the process of air oxidation. The results are presented in Figure 8. Three samples had a similar dehydration process before 100 °C. However, with the increase of temperature, the three samples showed completely different changes. Freshly prepared Pd/SiO₂ had the greatest mass increase, which should be related to the oxidation of metallic Pd⁰ to PdO. The mass

increase of f7 with the same mass was significantly smaller than that of freshly prepared Pd/SiO₂, while u7 with the same mass had no significant mass increase. f7 was composed of metallic Pd⁰ and Pd₄S, while u7 was mainly composed of PdO and Pd₄S. This stated that the mass increase of f7 was mainly related to the oxidation of metallic Pd⁰, while Pd₄S maintained sufficient oxidation stability even under temperature higher than 500 °C. This meant that Pd₄S could not be oxidized into palladium oxide nor into palladium sulfate. Therefore, it could be possible to conclude that in the low-temperature catalytic oxidation of methane, Pd₄S had sufficient stability to resist the oxidation of oxygen.

Table 3. Palladium species content of used catalysts with different H₂S concentration ^a.

Catalyst	Composition Ratio of Palladium Species (%)		
	Pd	PdO	Pd ₄ S
u0.2	5.3	59.5	35.2
u1	4.0	60.4	35.6
u3	5.9	54.2	39.9
u5	2.7	40.4	56.9
u7	3.1	36.6	60.3
u10	3.6	48.9	47.5

^a: Calculated by Pd fitted peak area by XPS.

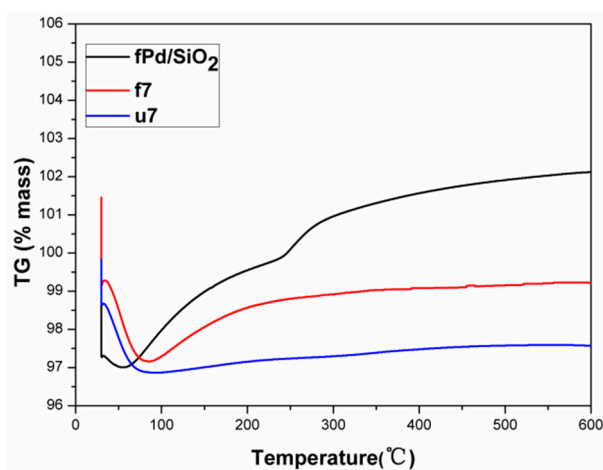


Figure 8. Temperature-programmed Oxidation (TPO) profiles of the (u7, f7) catalyst and freshly prepared Pd/SiO₂.

2.2.2. Activity Studies

Figure 9 covered the evaluation of the used catalysts and the evaluation method was completely consistent with the freshly prepared catalysts. To our delight, the sulfur-tolerance and catalytic activity of each used catalyst was almost unchanged with the fresh catalyst at 400 °C, which indicated that the composition of the catalyst had remained stable after the initial evaluation. The previous characterization results had confirmed that Pd₄S, PdO, and metal Pd⁰ were the three palladium species actually involved in the reaction. In the case that PdO and metal Pd⁰ did not have sulfur-tolerance, it was the existence of Pd₄S that gave the palladium active component the ability to resist the poisoning of sulfur species. Moreover, to our surprise, Pd₄S was not merely resistant to sulfur itself, its presence could even protect PdO and metal Pd⁰ from the poisoning of sulfur species.

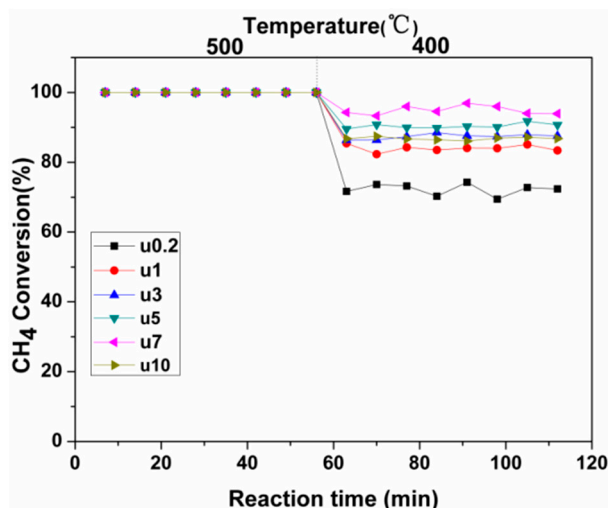


Figure 9. Catalytic performance of used catalysts with different H₂S concentration. Gas composition: CH₄ (v% = 2%), O₂ (v% = 8%), H₂S (v% = 0.02%), and N₂ (v% = 89.8%); Flow rate: 200 mL/min; and GHSV = 60000 mL/(g·h).

The sulfur-tolerance of the catalyst depended on Pd₄S, but it remained to be confirmed if catalytic activity was related to the type of palladium species. To this end, we correlated the relative amounts of Pd₄S and PdO species on the used catalyst surface with the catalytic activity of the used catalyst. The secondary reaction performance of the catalyst was selected at 400 °C and the results are shown in Figure 10. It could be noted that the variation of catalytic activity at 400 °C was closely related to the change of Pd₄S content with H₂S concentration increase. As the H₂S concentration increased from 0.2% to 7%, the relative content of Pd₄S and the catalytic activity of the used catalyst gradually increased. Compared with content change of (Pd₄S + PdO) and PdO, the content of (Pd₄S + PdO) did not change with the concentration of H₂S, but the change of PdO content was opposite to the catalytic activity of the used catalyst. The above results showed clearly that not only the sulfur-tolerance, but also the catalytic activity relied completely on Pd₄S. Because the coexistence of PdO did not play any decisive role, it was completely reasonable to use Pd₄S/SiO₂ as the catalyst prepared by the aqueous bubble sulfuration method. The consequences of 72-hour stability test of the u7 catalyst with and without H₂S are shown Figure 11. It could be found that the catalyst could maintain long-term stability regardless of the presence of H₂S in the reaction atmosphere.

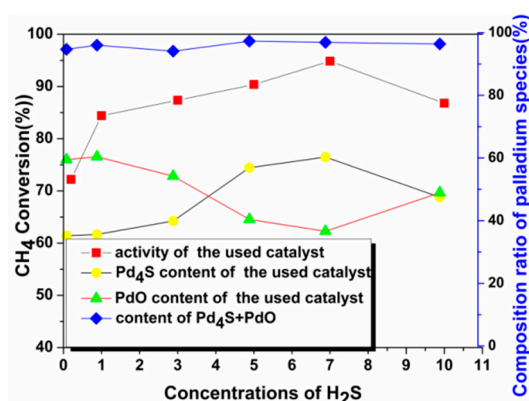


Figure 10. Relationship profile between composition ratio of Pd₄S and PdO on used catalysts and second evaluation of methane conversion. The composition ratio of palladium species was calculated through Pd fitted peak area by XPS.

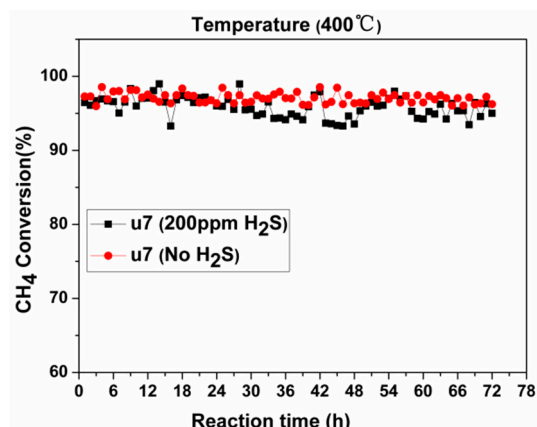


Figure 11. Long-term stability test of the u7 catalyst with and without H₂S. Gas composition: CH₄ (v% = 2%), O₂ (v% = 8%), H₂S (v% = 0.02%), and N₂ (v% = 89.8%); Flow rate: 200 mL/min; and GHSV = 60000 mL/(g·h).

2.3. Mechanism of Sulfur-Tolerance

Next, we turned to investigate the cause of sulfur-tolerance of the Pd₄S/SiO₂ using the technique of hydrogen sulfide temperature-programmed desorption (H₂S-TPD). The u7 catalyst and the freshly prepared PdO/SiO₂ catalyst were chosen for comparison and the results are presented in Figure 12. SO₂ and H₂S were the primary desorption species detected in the study. The PdO/SiO₂ catalyst released SO₂ in relatively large quantity, which suggested that PdO could readily assimilate H₂S to form PdO–SO_x. As a result, PdO/SiO₂ catalyst was poisoned and deactivated by H₂S. In contrast, desorption products were barely detected from the u7 catalyst. Seeing that Pd₄S was the only discrepancy between the two catalysts, i.e., the presence of Pd₄S in u7 and its absence in PdO/SiO₂, we were convinced that Pd₄S played a vital role in the sulfur-tolerance of u7 catalyst, as depicted in Scheme 1. Aside from not adsorbing H₂S, Pd₄S also prevented PdO from adsorbing H₂S onto its surface. Therefore, it was the Pd₄S that blocked the adsorption of H₂S and endowed the catalyst with sulfur-tolerance.

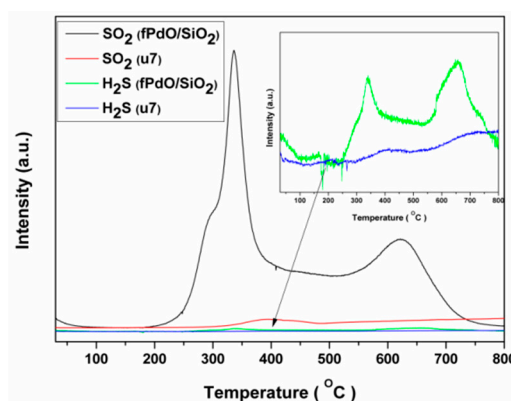
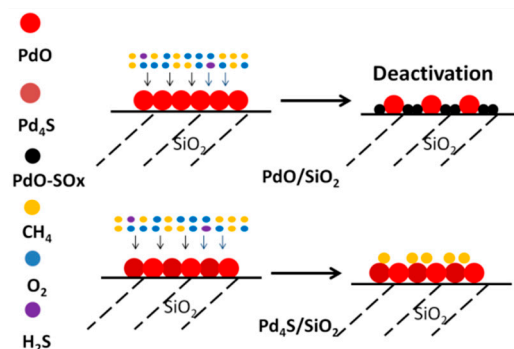


Figure 12. Hydrogen sulfide temperature-programmed desorption (H₂S-TPD) profiles of the u7 catalyst and freshly prepared PdO/SiO₂ catalyst.



Scheme 1. Schematic diagram of methane catalytic oxidation on the surface of Pd₄S/SiO₂ and PdO/SiO₂ in presence of H₂S.

3. Materials and Methods

3.1. Catalyst Preparation

The PdO/SiO₂ catalyst was prepared by isovolumetric impregnation. Typically, weigh a proper quantity of 40~60 mesh SiO₂ ($M = 10 \text{ g Vg} = 0.94 \text{ cm}^3/\text{g}$, $R_d = 10.6 \text{ nm}$, $S = 353.0028 \text{ m}^2/\text{g}$, Qingdao Baisha Catalyst Factory, Qingdao, China) was dispersed in palladium acetate (Aladdin Industrial Corporation, Shanghai, China) aqueous solution ($V_{\text{Pd}} = 0.05 \text{ g/mL}$) overnight. Then the sample was dried in an oven at 110 °C for 4 h and calcined at 500 °C for 4 h in the air. The theoretical loading of Pd was 5 wt. %.

The PdO/SiO₂ was first reduced to Pd/SiO₂ by H₂ at 500 °C for 1h. Pd_xS_y/SiO₂ catalyst was prepared by using above Pd/SiO₂ as precursor. 2.0 g Pd/SiO₂ and 100 ml deionized water were stirred at 350 rpm in a three-necked flask. Adjust the flow rate of H₂S and H₂ by flow controller (D07-19B, Beijing Sevenstart Electronics Co. Ltd, Beijing, China) to configure different concentrations of H₂S/H₂ mixture. Then 30 mL/min of H₂S–H₂ ($V_{\text{H}_2\text{S}}\% = 0.2, 1, 3, 5, 7, 10$) was fed into the suspension at 60 °C for 1 h. Afterwards, the sample was filtered and rinsed with distilled water till neutral. Finally, the sample was dried at 110 °C for 4 h. The freshly prepared catalyst is named (fV), and the used catalyst is named (uV), where V represents H₂S concentration.

3.2. Catalyst Characterization

X-Ray Diffraction (XRD) was carried out on a Thermo ARL X'TRA diffractometer (PNAlytical Co. Holland) using Cu K- α radiation (45 kV, 40 mA). Average particle size was determined from XRD measurements using the Scherrer formula:

$$d = \frac{K\lambda}{\beta \cos \theta'}$$

where d is the average particle size (nm), K is the Scherrer constant and the diffraction angle is denoted θ , $\lambda = 0.154 \text{ nm}$ stands for the wavelength of Cu K- α radiation, β denotes the full-width at half-maximum (FWHM) of diffraction peak.

High Resolution Transmission Electron Microscopy (HR-TEM) images were taken by a Philips-FEI Tecnai G2 F30 S-Twin transmission electron microscope operated at 300 kV (Philips-FEI Co. Holland).

X-Ray Photoelectron Spectroscopy (XPS) was measured on a Thermo ESCALAB 250 Axis Ultra (KRATOS, Kanagawa, Japan) using a monochromated Al K α X-ray source ($h\nu = 1485.6 \text{ eV}$) with a fixed analyzer pass energy of 80 eV. The binding energy values were referenced to the Si 2p as internal standard (Si 2p = 103.4 eV) and the maximum deviation value was 2.6 eV in the sample. After subtraction of the Shirley-type background, the core-level spectra were decomposed into their component with mixed Gaussian-Lorentzian lines by a non-linear least squares curve fitting procedure, using the public software package XPSPEAK4.1. The corresponding atomic ratio in different chemical

environment was obtained from the fitted XPS spectra of Pd 3d and S 2p. The XPS profiles were fitted by the software named "XPS peak". Then the fitting peak area was used to calculate the proportion of different species.

Temperature-programmed Oxidation (TPO) was performed on a NETZSCH STA 409 PC/PG instrument (NETZSCH Co. Selbc, Germany) The oxidation stability of the catalysts was investigated by recording the mass change in the process of air oxidation. TPO was performed by heating 0.01 g sample from room temperature to 600 °C in air atmosphere with a heating rate of 5 °C/min and a flow rate of 40 mL/min.

Temperature-programmed Desorption (TPD) of hydrogen sulfide experiments were performed in a self-made tubular quartz reactor (5mm i.d.). The sample (0.2 g) was first swept at 110 °C for 1 h using pure He and cooled to room temperature in the same atmosphere. Then the sample was in situ treated with H₂S (0.2% in N₂) at a flow rate of 30 mL/min for 0.5 h and swept 1 h to remove physisorbed and/or weakly bound species. TPD was performed by heating the sample from room temperature to 800 °C with constant increase of 5 °C/min in pure He. The TPD spectra were recorded by a quadrupole mass spectrometer (QMS 200 Omnistar, Pfeiffer Co. Germany).

3.3. Evaluation of Catalysts

The catalytic activity of the freshly prepared and used catalysts was tested with 0.2 g sample in a self-made continuous fixed bed reactor (8 mm i.d.) at atmospheric pressure. Gases consisting of CH₄ (v% = 2 %), O₂ (v% = 8 %), H₂S (v% = 0.02 %), and N₂ were fed through the flow controller (D07-19B, Beijing Sevenstart Electronics Co. Ltd., Beijing, China) at 200 mL/min and used in all the experiments. Finally, the temperature control controller (AI808PK1L2, XiaMen YuDian Automation Technology Co., Ltd., XiaMen, China) is used to control different reaction temperatures. The effluent gases were sampled and simultaneously analyzed online by gas chromatographs (GC-9790, Zhejiang Fuli Analytical Instruments Corp., Hangzhou, China). Exhaust gases were analyzed using a PoraPak Q column and a thermal conductivity detector (TCD). Methane conversions were calculated for outlet CO₂ concentrations.

4. Conclusions

Through the characterization of freshly prepared catalyst and used catalyst, we confirmed that Pd₄S, PdO, and metallic Pd⁰ were the actual palladium species involved in the oxidation of methane. Sulfur-tolerance and catalytic activity was completely dependent on Pd₄S, and independent on other palladium species. Moreover, Pd₄S had sufficient oxidation stability under reaction conditions. Therefore, even in the presence of PdO, there are enough reasons to represent the catalyst with Pd₄S/SiO₂. In summary, we have developed a powerful sulfur-tolerant catalyst for methane oxidation by incorporating Pd₄S into SiO₂, and to the best of our knowledge, this is the first report on Pd catalysts with such property. In view of the excellent sulfur-tolerant property, the excellent oxidation stability and the high catalytic activity, the Pd₄S/SiO₂ catalyst will definitely find valuable and versatile use in catalytic chemistry.

At the same time, as the Pd_xS_y species with the highest proportion of Pd/S, we cannot determine whether the outstanding performance of Pd₄S in methane catalytic oxidation is only a special case. Furthermore, sulfur-tolerant mechanism of Pd₄S needs further theoretical research.

Author Contributions: Conceptualization, L.M.; Data curation, S.Y. and H.Z.; Formal analysis, L.M., S.Y., and H.Z.; Funding acquisition, L.M. and C.L.; Investigation, T.J.; Methodology, X.Z.; Project administration, L.M. and X.L.; Writing—original draft, S.Y.; Writing—review & editing, L.M. and X.Z.

Funding: This work is financially supported by National Natural Science Foundation of China (Grant No.21473159, 21476208).

Conflicts of Interest: The authors declare no conflict of interest.

References

1. Trincherio, A.; Hellman, A.; Grönbeck, H. Methane oxidation over Pd and Pt studied by DFT and kinetic modeling. *Surf. Sci.* **2013**, *616*, 206–213. [[CrossRef](#)]
2. Mahara, Y.; Ohyama, J.; Tojo, T.; Murata, K.; Ishikawa, H.; Satsuma, K. Enhanced activity for methane combustion over a Pd/Co/Al₂O₃ catalyst prepared by a galvanic deposition method. *Catal. Sci. Technol.* **2016**, *6*, 4773–4776. [[CrossRef](#)]
3. Chen, J.; Arandiyana, H.; Gao, X.; Li, J. Recent Advances in Catalysts for Methane Combustion. *Catal. Surv. Asia* **2015**, *19*, 140–171. [[CrossRef](#)]
4. Colussi, S.; Gayen, A.; Camellone, M.F.; Boaro, M.; Llorca, J.; Fabris, S.; Trovarelli, A. Nanofaceted Pd-O Sites in Pd-Ce Surface Superstructures: Enhanced Activity in Catalytic Combustion of Methane. *Angew. Chem.* **2009**, *121*, 8633–8636. [[CrossRef](#)]
5. Ji, Y.; Guo, Y.B. Nanostructured perovskite oxides as promising substitutes of noble metals catalysts for catalytic combustion of methane. *Chin. Chem. Lett.* **2018**, *29*, 252–260.
6. Bossche, M.V.D.; Gronbeck, H. Methane Oxidation over PdO(101) Revealed by First-Principles Kinetic Modeling. *J. Am. Chem. Soc.* **2015**, *137*, 12035–12044. [[CrossRef](#)] [[PubMed](#)]
7. Monai, M.; Montini, T.; Gorte, R.J.; Fornasiero, P. Catalytic Oxidation of Methane: Pd and Beyond. *Eur. J. Inorg. Chem.* **2018**, *25*, 2884–2893. [[CrossRef](#)]
8. Jiang, L.; Zheng, Y.; Chen, X.; Xiao, Y.; Cai, G.; Zheng, Y.; Zhang, Y.; Huang, F. Catalytic Activity and Stability over Nanorod-Like Ordered Mesoporous Phosphorus-Doped Alumina Supported Palladium Catalysts for Methane Combustion. *ACS Catal.* **2018**, *8*, 11016–11028.
9. Fouladvand, S.; Skoglundh, M.; Carlsson, P.A. A transient in situ infrared spectroscopy study on methane oxidation over supported Pt catalysts. *Catal. Sci. Technol.* **2014**, *4*, 3463–3473. [[CrossRef](#)]
10. Florén, C.R.; Bossche, M.V.D.; Creaser, D.; Grobeck, H.; Carlsson, P.A.; Korpi, H.; Skoglundh, M. Modelling complete methane oxidation over palladium oxide in a porous catalyst using first-principles surface kinetics. *Catal. Sci. Technol.* **2018**, *8*, 508–520. [[CrossRef](#)]
11. Banerjee, A.C.; Golub, K.W.; Abdul, Md. H.; Billor, M.Z. Comparative study of the characteristics and activities of Pd/ γ -Al₂O₃ catalysts prepared by Vortex and Incipient Wetness Methods. *Catalysts* **2019**, *9*, 336. [[CrossRef](#)]
12. Banerjee, A.C.; McGuire, M.M.; Lawnick, O.; Bozack, M.J. Low-temperature activity and PdO/PdOx transition in methane combustion by a PdO-PdOx/ γ -Al₂O₃ catalyst. *Catalysts* **2018**, *8*, 266. [[CrossRef](#)]
13. Ciuparu, D.; Lyubovsky, M.R.; Altman, E.; Pfefferle, L.D.; Datye, A. Catalytic combustion of methane over palladium based catalysts. *Catal. Rev. Sci. Eng.* **2002**, *44*, 593–649. [[CrossRef](#)]
14. Persson, K.; Pfefferle, L.D.; Schwartz, W.; Ersson, A.; Jaras, S.G. Stability of palladium-based catalysts during catalytic combustion of methane: The influence of water. *Appl. Catal. B* **2007**, *74*, 242–250. [[CrossRef](#)]
15. Liu, Y.; Wang, S.; Gao, D.; Sun, T.; Zhang, C.; Wang, S.D. Influence of metal oxides on the performance of Pd/Al₂O₃ catalysts for methane combustion under lean-fuel conditions. *Fuel Process. Technol.* **2013**, *111*, 55–61. [[CrossRef](#)]
16. Baylet, A.; Royer, S.; Marecot, P.; Tatibouet, J.M.; Duprez, D. High catalytic activity and stability of Pd doped hexaaluminate catalysts for the CH₄ catalytic combustion. *Appl. Catal. B* **2008**, *77*, 237–247. [[CrossRef](#)]
17. Ma, J.; Lou, Y.; Cai, Y.; Zhao, Z.; Wang, L.; Zhan, W.; Guo, Y.; Guo, Y. The relationship between the chemical state of Pd species and the catalytic activity for methane combustion on Pd/CeO₂. *Catal. Sci. Technol.* **2018**, *8*, 2567–2577. [[CrossRef](#)]
18. Mihai, O.; Smedler, G.; Nylén, U.; Olofsson, M.; Olsson, L. The effect of water on methane oxidation over Pd/Al₂O₃ under lean, stoichiometric and rich conditions. *Catal. Sci. Technol.* **2017**, *7*, 3084–3096. [[CrossRef](#)]
19. Zi, X.; Liu, L.; Xue, B.; Dai, H.; He, H. The durability of alumina supported Pd catalysts for the combustion of methane in the presence of SO₂. *Catal. Today* **2011**, *175*, 223–230. [[CrossRef](#)]
20. Wilburn, M.S.; Epling, W.S. Sulfur deactivation and regeneration of mono- and bimetallic Pd-Pt methane oxidation catalysts. *Appl. Catal. B* **2017**, *206*, 589–598. [[CrossRef](#)]
21. Monai, M.; Montini, T.; Melchionna, M.; Ducchon, T.; Kus, P.; Chen, C.; Tsud, N.; Nasi, L.; Prince, K.C.; Veltruska, K.; et al. The effect of sulfur dioxide on the activity of hierarchical Pd-based catalysts in methane combustion. *Appl. Catal. B* **2017**, *202*, 72–83. [[CrossRef](#)]

22. Yin, F.; Ji, S.; Wu, P.; Zhao, F.; Liu, H.; Li, C. Preparation of Pd-Based Metal Monolithic Catalysts and a Study of Their Performance in the Catalytic Combustion of Methane. *ChemSusChem* **2008**, *1*, 311–319. [[CrossRef](#)]
23. Hoyos, L.J.; Praliaud, H.; Primet, M. Catalytic combustion of methane over palladium supported on alumina and silica in presence of hydrogen-sulfide. *Appl. Catal. A* **1993**, *98*, 125–138. [[CrossRef](#)]
24. Venezia, A.M.; Carlo, G.D.; Liotta, L.F.; Pantaleo, G.; Kantcheva, M. Effect of Ti(IV) loading on CH₄ oxidation activity and SO₂ tolerance of Pd catalysts supported on silica SBA-15 and HMS. *Appl. Catal. B* **2011**, *106*, 529–539. [[CrossRef](#)]
25. Ortloff, F.; Bohnau, J.; Kramar, U.; Graf, F.; Kolb, T. Studies on the influence of H₂S and SO₂ on the activity of a PdO/Al₂O₃ catalyst for removal of oxygen by total oxidation of (bio-)methane at very low O₂:CH₄ ratios. *Appl. Catal. B* **2016**, *182*, 550–561. [[CrossRef](#)]
26. Meezyoo, V.; Trimm, D.L.; Cant, N.W. The effect of sulfur containing pollutants on the oxidation activity of precious metals used in vehicle exhaust catalysts. *Appl. Catal. B* **1998**, *16*, L101–L104. [[CrossRef](#)]
27. Ordóñez, S.; Hurtado, P.; Díez, F.V. Methane catalytic combustion over Pd/Al₂O₃ in presence of sulfur dioxide: development of a regeneration procedure. *Catal. Lett.* **2005**, *100*, 27–34. [[CrossRef](#)]
28. Corro, G.; Cano, C.; Fierro, J.L.G. A study of Pt–Pd/γ-Al₂O₃ catalysts for methane oxidation resistant to deactivation by sulfur poisoning. *J. Mol. Catal. A: Chem* **2010**, *315*, 35–42. [[CrossRef](#)]
29. Simon, L.J.; Ommen, J.G.V.; Jentys, A.; Lercher, J.A. Sulfur-Tolerant Pt-Supported Zeolite Catalysts for Benzene Hydrogenation: I. Influence of the Support. *J. Catal.* **2001**, *201*, 60–69. [[CrossRef](#)]
30. Ferrer, I.J.; Diazchao, P.; Pascual, A.; Sánchez, C. An investigation on palladium sulphide (PdS) thin films as a photovoltaic material. *Thin Solid Films* **2007**, *515*, 5783–5786. [[CrossRef](#)]
31. Xu, W.; Ni, J.; Zhang, Q.F.; Feng, F.; Xiang, Y.Z.; Li, X.N. Tailoring supported palladium sulfide catalysts through H₂-assisted sulfidation with H₂S. *J. Mater. Chem. A* **2013**, *1*, 12811–12817. [[CrossRef](#)]
32. Zhang, Q.F.; Xu, W.; Li, X.N.; Jiang, D.H.; Xiang, Y.Z.; Wang, J.G.; Cen, J.; Romano, S.; Ni, J. Catalytic hydrogenation of sulfur-containing nitrobenzene over Pd/C catalysts: In situ sulfidation of Pd/C for the preparation of Pd_xS_y catalysts. *Appl. Catal. A* **2015**, *497*, 17–21. [[CrossRef](#)]
33. Mccue, A.J.; Guerrero-Ruiz, A.; Rodríguez-Ramos, I.; Anderson, J.A. Palladium sulphide – A highly selective catalyst for the gas phase hydrogenation of alkynes to alkenes. *J. Catal.* **2016**, *340*, 10–16. [[CrossRef](#)]
34. Menegazzo, F.; Canton, P.; Pinna, F.; Pernicone, N. Bimetallic Pd–Au catalysts for benzaldehyde hydrogenation: Effects of preparation and of sulfur poisoning. *Catal. Commun.* **2008**, *9*, 2353–2356. [[CrossRef](#)]
35. Mccue, A.J.; Anderson, J.A. Sulfur as a catalyst promoter or selectivity modifier in heterogeneous catalysis. *Cheminform* **2014**, *4*, 272–294. [[CrossRef](#)]
36. O'Brien, C.P.; Gellman, A.J.; Morreale, B.D.; Miller, J.B. The hydrogen permeability of Pd₄S. *J. Membr. Sci.* **2011**, *371*, 263–267. [[CrossRef](#)]
37. O'Brien, C.P.; Howard, B.H.; Miller, J.B.; Morreale, B.D.; Gellman, A.J. Inhibition of hydrogen transport through Pd and Pd₄₇Cu₅₃ membranes by H₂S at 350 degrees. *J. Membr. Sci.* **2010**, *349*, 380–384. [[CrossRef](#)]
38. Morreale, B.D.; Howard, B.H.; Iyoha, O.; Enick, R.M.; Ling, C.; Sholl, D.S. Experimental and Computational Prediction of the Hydrogen Transport Properties of Pd₄S. *Ind. eng. chem. res* **2007**, *46*, 6313–6319. [[CrossRef](#)]
39. Zubkov, A.; Fujino, T.; Sato, N.; Yamada, K. Enthalpies of formation of the palladium sulphides. *J. Chem. Thermodyn.* **1998**, *30*, 571–581. [[CrossRef](#)]
40. Iyoha, O.; Enick, R.; Killmeyer, R.; Morreale, B. The influence of hydrogen sulfide-to-hydrogen partial pressure ratio on the sulfidization of Pd and 70 mol% Pd–Cu membranes. *J. Membr. Sci.* **2007**, *305*, 77–92. [[CrossRef](#)]
41. Hensen, E.J.M.; Brans, H.J.A.; Lardinois, G.M.H.J.; deBeer, V.H.J.; vanVeen, J.A.R.; van Santen, R.A. Periodic Trends in Hydrotreating Catalysis: Thiophene Hydrodesulfurization over Carbon-Supported 4d Transition Metal Sulfides. *J. Catal.* **2000**, *192*, 98–107. [[CrossRef](#)]
42. Gerson, A.R.; Bredow, T. Interpretation of sulfur 2p XPS spectra in sulfide minerals by means of ab initio calculations. *Surf. Interface Anal.* **2000**, *29*, 145–150. [[CrossRef](#)]
43. Bhatt, R.; Bhattacharya, S.; Basu, R.; Singh, A.; Deshpande, U.; Surger, C.; Basu, S.; Aswal, D.K.; Gupta, S.K. Growth of Pd₄S, PdS and PdS₂ films by controlled sulfurization of sputtered Pd on native oxide of Si. *Thin Solid Films* **2013**, *539*, 41–46. [[CrossRef](#)]
44. Senftle, T.P.; Van Duin, A.C.T.; Janik, M.J. The Role of Site Stability in Methane Activation on Pd_xCe_{1-x}O_δ Surfaces. *ACS Catal.* **2015**, *5*, 6187–6199. [[CrossRef](#)]

45. Beketov, G.; Heinrichs, B.; Pirard, J.P.; Chenakin, S.; Kruse, N. XPS structural characterization of Pd/SiO₂ catalysts prepared by cogelation. *Appl. Surf. Sci.* **2013**, *287*, 293–298. [[CrossRef](#)]
46. Romanchenko, A.S.; Mikhlina, Y.L. An XPS study of products formed on pyrite and pyrrhotine by reacting with palladium (II) chloride solutions. *J. Struct. Chem.* **2015**, *56*, 531–537. [[CrossRef](#)]
47. Corro, G.; Vázquez-Cuchillo, O.; Banuelos, F.; Fierro, J.L.G.; Azomoza, M. An XPS evidence of the effect of the electronic state of Pd on CH₄ oxidation on Pd/gamma-Al₂O₃ catalysts. *Catal. Commun.* **2007**, *8*, 1977–1980. [[CrossRef](#)]
48. Chenakin, S.P.; Melaet, G.; Szukiewicz, R.; Kruse, N. XPS study of the surface chemical state of a Pd/(SiO₂+TiO₂) catalyst after methane oxidation and SO₂ treatment. *J. Catal.* **2014**, *312*, 1–11. [[CrossRef](#)]
49. Weng, X.; Ren, H.; Chen, M.; Wan, H. Effect of Surface Oxygen on the Activation of Methane on Palladium and Platinum Surfaces. *ACS Catal.* **2014**, *4*, 2598–2604. [[CrossRef](#)]
50. Cargnello, M.; Jaén, J.J.D.; Garrido, J.C.H.; Bakhmutsky, K.; Montini, T.; Gámez, J.J.C.; Gorte, R.J.; Fornasiero, P. Exceptional Activity for Methane Combustion over Modular Pd@CeO₂ Subunits on Functionalized Al₂O₃. *Science* **2012**, *337*, 713–718. [[CrossRef](#)] [[PubMed](#)]
51. Widjaja, H.; Sekizawa, K.; Eguchi, K.; Arai, H. Oxidation of methane over Pd/mixed oxides for catalytic combustion. *Catal. Today* **1999**, *47*, 95–101. [[CrossRef](#)]
52. Sekizawa, K.; Widjaja, H.; Maeda, S.; Ozawa, Y.; Eguchi, K. Low temperature oxidation of methane over Pd catalyst supported on metal oxides. *Catal. Today* **2000**, *59*, 69–74. [[CrossRef](#)]



© 2019 by the authors. Licensee MDPI, Basel, Switzerland. This article is an open access article distributed under the terms and conditions of the Creative Commons Attribution (CC BY) license (<http://creativecommons.org/licenses/by/4.0/>).